Classification of Time Series Data Obtained by the Satellite by Using Rule-Based and Machine-Learning Methods

Satoko Saita
National Institute of Technology, Kitakyushu College, 5-20-1 Shii, Kokuraminamiku, Kitakyushu, Fukuoka, 802-0985 Japan

Mariko Teramoto
Faculty of Engineering, Kyushu Institute of Technology, 1-1 Sensui-Cho, Tobata, Kitakyushu, Fukuoka, 804-8550

Kentarou. Kitamura
Faculty of Engineering, Kyushu Institute of Technology, 1-1 Sensui-Cho, Tobata, Kitakyushu, Fukuoka, 804-8550

E-mail: saita@kct.ac.jp
researchmap.jp/saita

Abstract

Because of its communication volume constraints, scientific observations by nanosatellites need to reduce downlink data by onboard data preprocessing. Therefore, we tried to classify time series data of the geomagnetic field obtained by the SWARM satellite to determine the most appropriate method for onboard classification of a phenomenon in the geomagnetic field. The classifications have been executed using rule-based, K-means, and combined CNN methods. The experimental results demonstrated the effectiveness of the machine-learning model with LSTM networks.

Keywords: Deep-Learning, Nanosatellite, Machine-Learning, Time-series Classification

1. Introduction

It is known that electromagnetic waves occurring in geospace are affected by the near-earth plasma environment. Among those, the electromagnetic ion cyclotron (EMIC) waves are generated by the cyclotron-resonant instability of the anisotropic energetic (10 – a few 100 keV) protons [1], [2]. In the Earth's magnetosphere, the EMIC waves can be dealt with in the ULF (Ultra-low Frequency) range (0.1 - 5 Hz).

The electrons can resonate with the EMIC waves, and the energy of the electrons may go up to 50 MeV. The electrons in the MeV energy range can affect neural dynamics [3], [4].

Therefore, studies of EMIC waves are essential for a better understanding of their overall role in the interaction of the solar wind with the Earth's magnetosphere-ionosphere-atmosphere coupled system.

In general, magnetic measurements to monitor the populations of EMIC waves along their orbits have been conducted by conventional satellites with a weight of more than 100 kg. On the other hand, nanosatellites with

a weight of less than 50 kg are exponentially increasing since 2013. Therefore, they are expected to be a potential candidate for affordable tool in-orbit observation for the sciences (Esper et al., 2000) [15]. The Laboratory of Lean Satellite Enterprises and In-orbit Experiments (LaSEINE), established by the Kyushu Institute of Technology, is developing these nanosatellites. One of the most expected outcomes of the development is an enhancement of geomagnetic pulsation (including EMIC waves) observations. However, the observation by nanosatellites is required to reduce the downlink data because the miniaturization of the satellites constrains their communication capabilities.

To reduce the downlink data, preliminary data analysis should be done in orbit, and the minimum required data already analyzed can be downlinked to the ground station. In this paper, we developed deep-learning and rule-based methods to detect geomagnetic pulsations. This study will provide a system to evaluate the EMIC-wave-appearance period. Furthermore, this study will contribute to creating a system that allows more downlink data of a particular period, such as specific geomagnetic pulsations.

2. Materials and Methodology

2.1. *Data Preparation*

Geomagnetic field data obtained from satellites are used for this study. Swarm, the European Space Agency's first constellation mission for Earth Observation, consists of three satellites for the Earth's magnetic field observation. The identical satellites Alpha, Bravo, and Charlie (A, B, and C) were launched on 22 November 2013 into a near-polar orbit with orbital inclinations of 87.4° for Swarm-A and -C and 88.0° for Swarm-B. In this study, we utilized high-resolution vector magnetic field data sampled at 50 Hz with an accuracy of 0.01 nT from the satellite “A” during the magnetic storm of 22 June 2015.

The fluctuating field was then expressed in the field-aligned coordinate system, in which the ***z***-axis is parallel to the background magnetic field lines (***B***), the ***y***-axis is defined as (***B*** x ***R***), where ***R*** is the radial vector from the Earth's center to the satellite location, and ***x***-axis corresponds to $\boldsymbol{y} \times \boldsymbol{z}$. By and Bx points toward the geomagnetic east and upward, respectively.

To determine the background magnetic field, we applied a Savitzky-Golay smoothing filter with a window

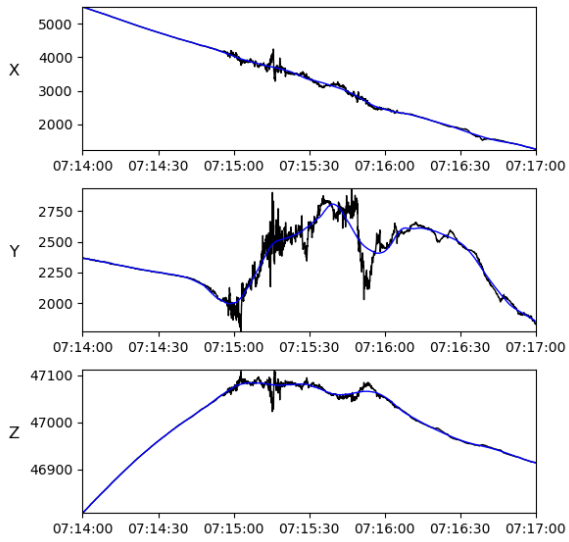

Fig. 1. Original data (black) and smoothing data (blue) of the 50-Hz magnetic field

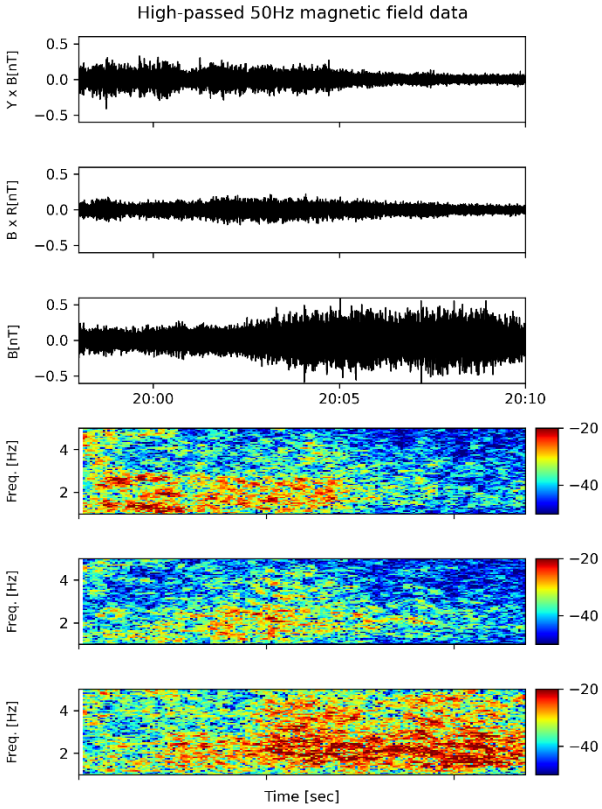

Fig. 2. High-passed 50 Hz magnetic field component in the mean-field-aligned coordinates.

of 30 x 50 data points and a second-order polynomial [5]. Above stated method was also used by Kim et al. (2018) and Wang et al. (2019) [6], [7]. Fig. 1 shows the original 50-Hz data (black) and the smoothing data (blue). An example wave spectrogram is shown in Fig. 2. The top three panels show the temporal variations of the fluctuating magnetic field in the field-aligned coordinate system as observed by Swarm A from 19:58 to 20:10 universal time (UT) on 22 June 2015. The cutoff frequency for a high-pass filter is 0.1 Hz. Examples of detected EMIC waves observed by Swarm A on 22 June 2015. The bottom three panels of Fig. 2 show the results of the spectrogram analysis. The fast Fourier transform (FFT) was performed with a window size of 800 data points (~16 s) and an overlap of 600 points (~12 s).

In previous studies, we need visual checks of FFT spectra to identify EMIC wave events because other electromagnetic activities might contaminate the fluctuating magnetic field data, including the signal of EMC waves. We can determine that EMIC wave events can be detected based on the following criteria: the signals satisfy at least 0.15 Hz bandwidth and at least 1 min duration. Then we can also exclude the other type of pulsations or background noises classified with amplitudes of bottom frequency [8].

The magnetic field data obtained from satellite "A" had been normalized, standardized, and reshaped to construct machine-learning datasets. First, these time series data are split into 6000 data points and labeled with "EMIC wave appearing (1)" or "no EMIC wave appearing (0)". Then we split fragmented data for training, validation, and testing datasets.

2.2. *Machine Learning*

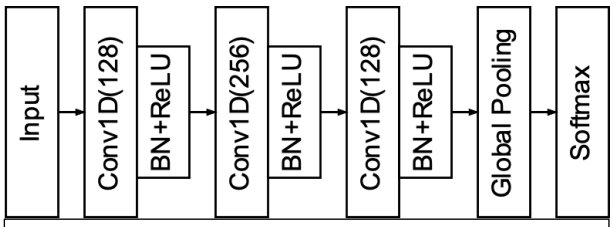

Fig. 3. The basic design of the fully convolutional network model.

This study used the fully convolutional network model to determine EMIC wave events [9], [11]. Fig. 3 shows the architecture of the fully convolutional network model. This model uses CNNs to extract image features, then transforms the number of channels into the number of classes via a convolutional layer, and finally converts the height and width of the feature map to those of the input image via the transposed convolution. As a result, the model output has the same size as the input data.

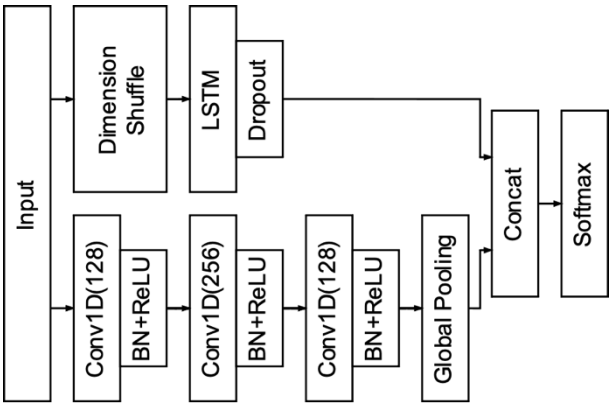

Fig. 4. Architecture of the 1d-CNN + LSTM model. In this architecture, the shortcut connections are used to pass information from the downsampling layers to the upsampling layers.

A model consisting of convolutional neural networks (CNNs) and long short-term memory networks (LSTM) was also applied to the datasets. In the model, the fully convolutional block is augmented by a Long Short Time Memory block [12]. The fully convolutional block consists of three stacked temporal convolutional blocks. Each convolutional block is identical to the convolution block in the CNN architecture. Each block consists of a temporal convolutional layer, accompanied by batch normalization followed by a ReLU (Rectified Linear Unit) activation function. Finally, global average pooling is applied following the final convolution block. Simultaneously, the time series input is conveyed into a dimension shuffle layer. The transformed time series from the dimension shuffle is passed into the LSTM block. The LSTM block comprises either a general LSTM layer or an Attention LSTM layer. Fig. 4 shows the architecture of the 1d-CNN + LSTM model. This method is a new approach for extracting EMIC waves. In this case, we proposed a method for acquiring spectrograms. We provided an example of pre-processing time series data for a group of training datasets needed in this case.

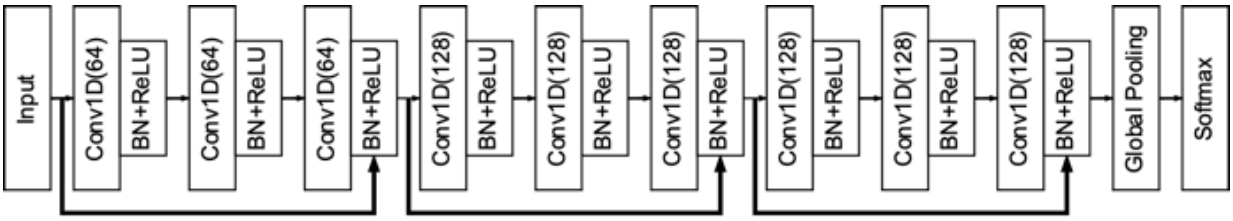

Fig. 5. Architecture of the Residual Network

We also applied the Residual Network model to determine EMIC wave events. ResNet was developed by He et al. 2016 [13]. Fig. 5 shows the architecture of the Residual Network. The advantage of the ResNets model compared to other architectural models is that the performance of this model does not decrease even though the architecture is getting deeper. The ResNet model is implemented by skipping connections on two to three layers containing ReLU and batch normalization among the architectures. He et al. showed that the ResNet model performs better in image classification than other models, indicating that the image features were extracted well by ResNet.

2.3. *Data Visualization*

We used Class Activation Maps (CAMs) to visualize where the model paid attention. CAMs enable us to see not only the class the network predicts but also the part of the image the network is especially interested in (Zhou et. al., 2015). The visualization provides a powerful way to communicate data-driven findings, motivate analyses and detect flaws. Fig. 6 shows an example of applying CAMs to the magnetic field data. The left figure shows the result of the Class Activation Mapping. We can see that the CNN network pays attention to about a frequency range, which is consistence with the eigenfrequencies of geomagnetic pulsations. The data analysis and machine learning were performed in accordance with Nielsen (2019) [14].

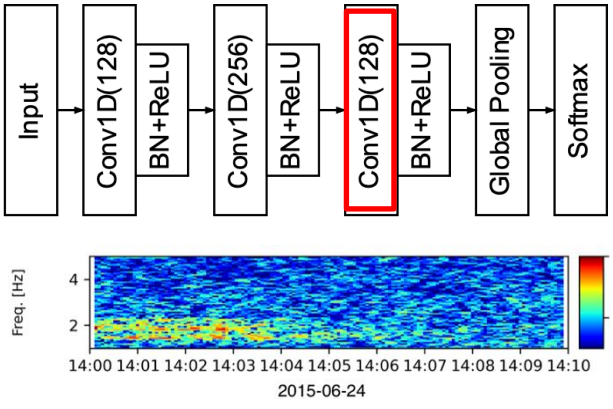

Fig. 6. The example of the results of Class Activation Maps (CAMs).

3. Results

In this study, we applied machine learning to the time series data obtained from SWARM satellites. This study aimed to develop a satellite system to discriminate specific natural phenomena in a future mission. The observation data of the SWARM satellites were assumed as magnetic field data observed by a CubeSat, and the model was trained. The SWARM satellites are scientific satellites for measuring the earth's magnetic field and were launched in 2013 by ESA [10]. The magnetic field data observed by SWARM are available to the public and can be acquired via the Internet.

Table 1. Comparison of accuracy in several testing datasets for machine learning models.

Kind of data	1DCNN-LSTM	FCN	ResNet
line plot	72.6	72.3	73.4
spectrogram	79.6	79.6	80.2

We use 2 kinds of input data and applied 3 machine learning models to identify EMIC wave events. ResNet applied to both kind of data shows the highest accuracy. The results using spectrograms show good performance on all of the machine learning models (Table 1).

4. Conclusions

We got the results by using the data separated every 600 seconds. However, these results also include possibilities for improvement. the correct answer rate is expected to be improved when the data of 300 seconds was prepared in the 60-second unit and the learning data was increased by 10 times. And this study addresses only a few EMIC wave events. We must continue to accumulate EMIC wave events and build a rich data set. In the forthcoming works, we will propose incorporating added architectures with their variants using the corresponding datasets.

Acknowledgements

This work was done in the framework of joint studies between the Kyushu Institute of Technology and KOSEN.

References

1. Cornwall JM (1965) Cyclotron instabilities and electromagnetic emission in the ultra low frequency and very low frequency ranges. J Geophys Res 70(1):61–69
2. Kennel CF, Petschek H (1966) Limit on stably trapped particle fluxes. J Geophys Res 71(1):1–28
3. Meredith NP, Thorne RM, Horne RB, Summers D, Fraser BJ, Anderson RR (2003), Statistical analysis of relativistic electron energies for cyclotron resonance with emic waves observed on crres. J Geophys Res 108:A6
4. Tsurutani B, Hajra R, Tanimori T, Takada A, Remya B, Mannucci A, Lakhina G, Kozyra, J, Shiokawa K, Lee L et al (2016) Heliospheric plasma sheet (hps) impingement onto the magnetosphere as a cause of relativistic electron dropouts (reds) via coherent emic
5. Savitzky, A. and Golay, M. J. E. (1964). Smoothing and differentiation of data by simplified least squares procedures. Analytical Chemistry, 36(8), 1627–1639. https://doi.org/10.1021/ac60214a047
6. Wang, H., He, Y. F., Lühr, H., Kistler, L., Saikin, A., Lund, E., & Ma, S. (2019). Storm time EMIC waves observed by Swarm and Van Allen Probe satellites. Journal of Geophysical Research: Space Physics, 124, 293– 312.
7. Kim, H., Hwang, J., Park, J., Bortnik, J., & Lee, J. (2018). Global characteristics of electromagnetic ion cyclotron waves deduced from Swarm satellites. Journal of Geophysical Research: Space Physics, 123, 1325– 1336.
8. Erlandson, R. E., & Anderson, B. J. (1996). Pc 1 waves in the ionosphere: A statistical study. Journal of Geophysical Research, 101(A4), 7843–7857.
9. Zhou, B., Khosla, A., Lapedriza, A., Oliva, A., and Torralba, A., "Learning Deep Features for Discriminative Localization", *arXiv e-prints*, 2015.
10. Friis-Christensen, E., H. Lühr, D. Knudsen, R. Haagmans (2007), Swarm – An Earth Observation Mission investigating Geospace, Advances in Space Research, Volume 41, Issue 1, 2008, Pages 210-216, ISSN 0273-1177.
11. Long, J., Shelhamer, E., & Darrell, T. (2015). Fully convolutional networks for semantic segmentation. Proceedings of the IEEE conference on computer vision and pattern recognition (pp. 3431–3440).
12. Karim MA, et al. (2018). Distinct features of multivesicular body-lysosome fusion revealed by a new cell-free content-mixing assay. Traffic 19(2):138-149.
13. He, K., Zhang, X., Ren, S., & Sun, J. (2015). Deep Residual Learning for Image Recognition. 2016 IEEE Conference on Computer Vision and Pattern Recognition (CVPR), 770-778.
14. Nielsen, A.(2019), Practical Time Series Analysis: Prediction with Statistics and Machine Learning, O'Reilly Media, ISBN: 9781492041627.
15. Esper J, P. V. Panetta, M. Ryschkewitsch, W. Wiscombe, and S. Neech, NASA-GSFC nano-satellite technology for Earth Science Missions, Acta Astronautica, 46, 2-6, 287-296, 2000

Authors Introduction

Dr. Satoko Saita

She is an Associate Professor of the Department of Creative Engineering at the National Institute of Technology, Kitakyushu College in Japan. She graduated from the Department of Earth and Planetary Sciences, Kyushu University, in 2000. She received his Ph.D. degree in Science from Kyushu University in 2005. Her research interest is Space and Upper Atmospheric Sciences.

Dr. Mariko Teramoto

She is an Associate Professor at the Faculty of Engineering at Kyushu Institute of Technology in Japan.
She received the B.S., M.S., and Ph.D. degrees from the Department of Geophysics, Kyoto University, Kyoto, Japan, in 2005, 2007, and 2010 respectively. Her research interest is geomagnetic variations and dynamics of plasmas in geospace.

Dr. Kentaro Kitamura

He is a Professor at the Faculty of Engineering at Kyushu Institute of Technology in Japan. He graduated from the Department of Earth and Planetary Sciences, Kyushu University, in 1997. He received his Ph.D. degree in Science from Kyushu University in 2001. His research interest is Space Weather and nano-satellite.